

Communication

Including Liquid Metal into Porous Elastomeric Films for Flexible and Enzyme-Free Glucose Fuel Cells: A Preliminary Evaluation

Denis Desmaële ^{1,*},†, Francesco La Malfa ^{1,2,†}, Francesco Rizzi ¹ , Antonio Quattieri ¹
and Massimo De Vittorio ^{1,2,*}

¹ Istituto Italiano di Tecnologia (IIT), Center for Biomolecular Nanotechnologies, Via Barsanti, 73010 Arnesano, Italy; francesco.lamalfa@iit.it (F.L.M.); francesco.rizzi@iit.it (F.R.); antonio.quattieri@iit.it (A.Q.)

² Dipartimento di Ingegneria dell'Innovazione, Università del Salento, 73100 Lecce, Italy

* Correspondence: denis.desmaele@iit.it (D.D.); massimo.devittorio@iit.it (M.D.V.); Tel.: +39-0832-1816-241 (D.D.)

† These authors contributed equally to this work.

Received: 18 October 2018; Accepted: 14 November 2018; Published: 22 November 2018



Abstract: This communication introduces a new flexible elastomeric composite film, which can directly convert the chemical energy of glucose into electricity. The fabrication process is simple, and no specific equipment is required. Notably, the liquid metal Galinstan is exploited with a two-fold objective: (i) Galinstan particles are mixed with polydimethylsiloxane to obtain a highly conductive porous thick film scaffold; (ii) the presence of Galinstan in the composite film enables the direct growth of highly catalytic gold structures. As a first proof of concept, we demonstrate that when immersed in a 20 mM glucose solution, a 5 mm-long, 5 mm-wide and 2 mm-thick sample can generate a volumetric power density up to $3.6 \text{ mW}\cdot\text{cm}^{-3}$ at $7 \text{ mA}\cdot\text{cm}^{-3}$ and 0.51 V without using any enzymes.

Keywords: Galinstan; liquid metal; porous gold; glucose fuel cell; enzyme-free

1. Introduction

Considering the ever-increasing demand for thin, lightweight and compliant electronic systems, recent research efforts have been made to develop correspondingly miniature power sources (e.g., see [1] and the references therein). For healthcare- and/or biomedical-related applications, bioelectrochemical energy sources are an attractive option. Efforts in this field, however, have predominantly focused on the development of enzyme-based configurations [2–4]. Enzymes can for instance be efficiently employed to generate a useful amount of electricity from lactate [5,6] or glucose [7,8] at concentrations that can be found in body fluids (e.g., sweat, blood, tears, etc.). Nonetheless, it is well recognized that the limited stability of enzymes poses great challenges for applications targeting long periods of operation (e.g., cardiac pacemakers) [9,10]. Alternatively, porous gold (PG) appears as a promising option for developing new electrodes featuring longer term stability. PG can indeed directly convert the chemical energy of glucose into electricity without using enzymes [11]. The hydrogen-assisted electrodeposition technique (HAET) is one of the fastest and most affordable methods recently discussed to fabricate PG electrodes [12]. Most works that discussed the HAET, however, reported PG electrodes with rather small geometrical dimensions [11,13]. To the best of our knowledge, the possibility to upscale the HAET to fabricate enzyme-free PG electrodes that could meet the power budget of real electronic devices remains to be demonstrated.

In this perspective, the liquid metal Galinstan might offer an alternative to the HAET for creating PG electrodes. Galinstan is a room temperature eutectic alloy composed of gallium, indium and

tin. Beyond the fact that Galinstan is highly conductive and can be used to create innovative flexible/stretchable electronic systems (e.g., see the applications and examples reviewed in [14]), another distinctive feature of Galinstan is that it can be exploited to create liquid metal marbles; namely, its silvery surface can be covered with different micro-/nano-particles or powders [15–17], including gold structures [18].

Based on these recent findings, this short communication explores the possibility to fabricate new PG electrodes by using Galinstan. Here, the use of Galinstan is two-fold. Firstly, Galinstan inclusions are embedded into polydimethylsiloxane (PDMS) to fabricate a highly conductive porous elastomeric composite scaffold. Secondly, the presence of Galinstan in the porous composite scaffold is exploited to grow complex gold structures that can directly generate electricity when immersed in a glucose solution.

2. Materials and Methods

Unless otherwise stated, all chemicals were obtained from Sigma-Aldrich (Milan, Italy) and used as received.

2.1. Fabrication of the Conductive Porous Elastomeric Scaffold

In a first step, Galinstan was mixed with PDMS (Sylgard 184, Dow Corning) in a way similar to the one reported in [19]. Briefly, PDMS was first prepared in a 1:10 ratio of curing agent and PDMS monomer. After degassing, 1 g of PDMS was gently mixed with 6.6 g of Galinstan (62% gallium, 22% indium and 9% tin by weight, Smart-elements) during 3–5 min until a homogenous viscous gray composite was observed. About 1.5 g of the PDMS/Galinstan mixture was poured in a square plastic box ($2.5 \times 2.5 \times 0.64$ cm) used as a mold. The box was gently inclined in all directions to obtain a visually uniform layer. Compared to the protocol reported in [19], the additional following steps were required to obtain a porous film. White sugar grains (average diameter estimated as ≈ 581 μm , $n = 15$) were poured onto the PDMS/Galinstan film. The box was placed under vacuum for 5 min to increase the penetration of the sugar grains into the composite. The sample was then placed in a thermostatic oven (G-therm, Fratelli Galli) and heated at 60 $^{\circ}\text{C}$ for 1 h. The resulting solidified thick film encompassing PDMS/Galinstan and sugar was detached from the box and placed in a beaker containing ≈ 200 mL of water. The beaker was covered with a paraffin film (Parafilm M) and positioned onto a hot plate (C-MAG HS7, IKA, Staufen, Germany) set to 80 $^{\circ}\text{C}$. It was heated overnight under continuous stirring to dissolve the sugar grains. The beaker was subsequently placed in a sonicator bath (Sonorex Digitec DT106, Bandelin, Germany) for 1 h with the initial aim to remove any sugar residues that might still be entrapped in the PDMS/Galinstan. At the end of the sonication process, the water became grayish. The PDMS/Galinstan film was finally placed under a fume hood at room temperature until complete drying.

2.2. Incorporation of the PG

For preliminary tests, only a small electrode was prepared. To that end, a small piece (SP) of the PDMS/Galinstan film was cut with a scalpel. The SP cut was 5 mm long, 5 mm wide and 2 mm thick. It was subsequently placed in a custom-made PDMS reservoir containing 2 mL of a 10 mM solution of gold (III) chloride trihydrate (HAuCl_4). It is noteworthy that we used here a concentration of HAuCl_4 ten-times lower when compared to other works (e.g., [11]). A thin black-colored layer appeared on the SP after a few minutes of coming in contact with the HAuCl_4 solution. During the reaction, the latter turned progressively from yellow to transparent. After ≈ 3 h, a faintly reddish-brown color started to appear, and the SP was removed from the reservoirs. The final small PG electrode (SPGE) obtained was dried overnight at room temperature prior to further tests.

2.3. Microstructure Characterization and Instrumentation

The morphology of both the porous PDMS/Galinstan film and the SPGE was analyzed using a scanning electron microscope (SEM, Helios NanoLab 600i, FEI). A layer of gold (≈ 5 nm) was deposited onto the samples (Q150RS, Quorum) in order to enhance the quality of the images. Measures of electrical resistance of the PDMS/Galinstan were performed using a digital multimeter equipped with test leads (IDM 103N, ISO-TECH). For the electrochemical measurements, a stock solution of glucose (20 mM) was prepared in a neutral phosphate buffer and allowed to mutarotate overnight before use. This concentration was favored because it is representative of the glucose content that can be found in the human body. Particularly, it mimics the glucose content in blood for pathological (hyperglycemic) conditions [20,21]. The SPGE was used to catalyze glucose oxidation. It was immersed with a platinum cathode (10×25 mm) in a beaker filled with 15 mL of the glucose solution. Platinum was selected because it exhibits one of the highest oxygen reduction potentials in phosphate buffer pH 7 [22,23]. Polarization curve measurements were performed at room temperature (≈ 20 °C) using a potentiostat (Autolab, Eco chemie).

3. Results and Discussion

The porous PDMS/Galinstan obtained (film thickness ≈ 2 mm) is presented in Figure 1. Because the sugar was solely poured and not thoroughly mixed with the PDMS/Galinstan, the grains roughened mainly the top surface of the film (i.e., the bottom surface was still a plain thin layer; see the inset in Figure 1A). As can be seen in Figure 1B, however, the composite film featured a high degree of flexibility.

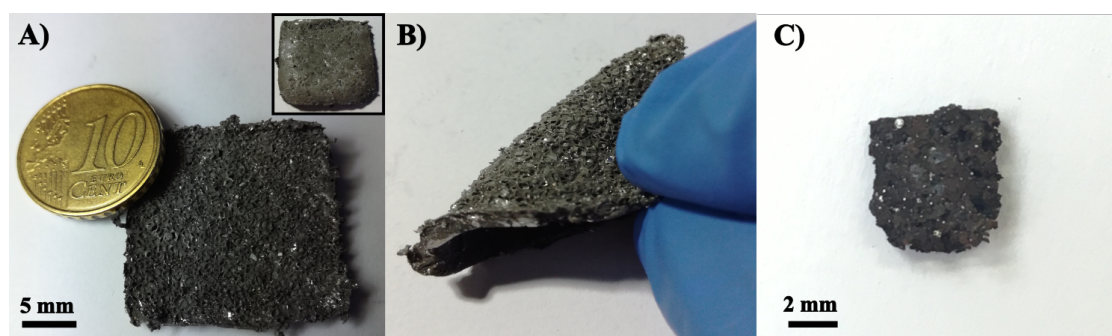


Figure 1. (A) Top view of the porous PDMS/Galinstan thick film (inset shows the backside of the sample); (B) image illustrating the flexibility of the PDMS/Galinstan composite; (C) top view of the black-colored small porous gold electrode (SPGE) decorated with PG.

Normally, liquid metal inclusions in non-porous PDMS matrices do not inherently lead to conductive elastomeric composites. One way to create localized conductive paths is to use mechanical sintering, namely the application of a punctual mechanical force causes Galinstan droplets to rupture and form electrical connections with neighboring inclusions [19]. On the contrary, we here noticed that a high level of conductivity could be achieved without applying a concentrated surface pressure. We indeed measured electrical resistance values ranging from $\approx 0.5 \Omega$ to $\approx 6 \Omega$ across the whole top (i.e., porous) surface of the sample shown in Figure 1A,B. Comparatively, we obtained a much higher electrical resistance by using a porous support matrix made of PDMS and carbon nanofibers to create another sponge-like electrode [24]. We presently hypothesize that we here obtained a good conductivity because two necessary conditions were met:

1. Sugar grains were utilized to create pores on the composite surface. It is likely that when the grains penetrated into the PDMS/Galinstan, they actually came into contact and formed connections with Galinstan inclusions. Although further investigation is required to better understand the exact underlying mechanism, we postulate that the removal of the sugar grains enabled Galinstan

- dispersions to reconnect and exit the composite pores. SEM images analysis indeed revealed the presence of Galinstan droplets in the vicinity of the pores (see Figure 2A).
2. A sonication step was performed at the end of the fabrication process. Although Figure 2A shows the presence of Galinstan droplets on the rough surface of the composite film, they remained isolated. As such, they could not form conductive paths. Nevertheless, we discovered that the sonication step we initially performed to ensure a complete removal of sugar residues actually broke the Galinstan. Liquid metal nanoparticles were previously created using sonication [25]. In our case, we observed the formation of thin films of Galinstan, which could spread across wide surface areas (Figure 2B,C). Although the surface of the porous PDMS/Galinstan was not entirely recovered by a continuous Galinstan thin film, multiple interconnected conductive paths were created. It is likely that the morphology of the Galinstan thin films created was influenced by the sonication power. Additionally, the sonication power might have played a critical role in the amount of Galinstan inclusions that could be extracted from the PDMS/Galinstan matrix. Indeed, it stands to reason that powerful ultrasound might alter the PDMS surface and release additional Galinstan when compared to the initial amount released by the sugar grains. Further investigation into the role of the sonication power will be conducted in the near future.

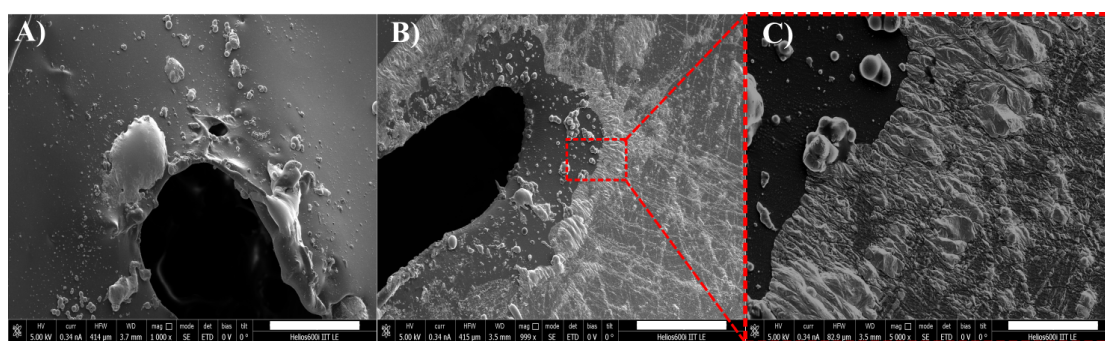


Figure 2. SEM micrographs of the porous PDMS/Galinstan thick film (see Figure 1A,B): (A) presence of Galinstan droplets around a pore of the composite after the removal of the sugar grain (scale bar is 100 μm); (B) view showing the creation of a continuous conductive thin film of Galinstan (right part of the image) after sonication (scale bar is 100 μm); (C) magnified view of the conductive thin film surface: the typical high roughness (wrinkles) of the Galinstan oxide skin is clearly visible (scale bar is 20 μm).

Figure 3A demonstrates that the thin films of Galinstan created after sonication could be exploited to grow PG. As seen in Figure 3B, highly branched gold structures appeared on the surface of the SPGE. Interestingly, we observed feather-like structures similar to those reported by the HAET, even though we used a concentration of HAuCl_4 ten-times lower [11]. The numerous sharp edges of such dendrites can drastically enhance catalytic activities [26–28].

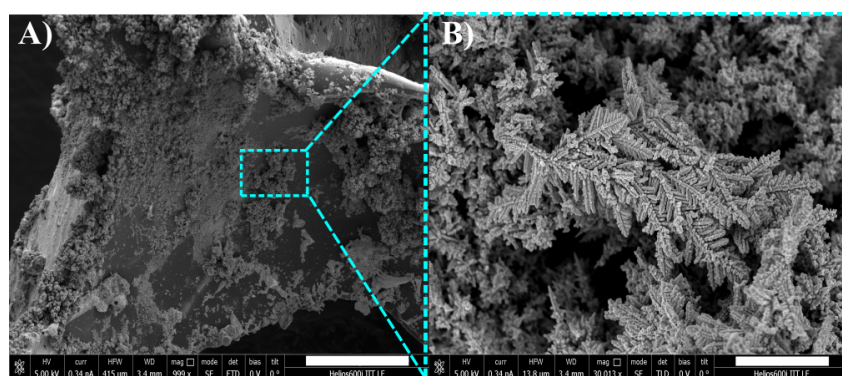


Figure 3. SEM micrographs of the SPGE covered with PG (see Figure 1C): (A) PG obtained after immersion of the porous PDMS/Galinstan in a HAuCl_4 solution (scale bar is 100 μm); (B) magnified view of gold dendrites obtained (scale bar is 3 μm).

The performance of SPGE was then evaluated. Figure 4 shows the polarization curve (i.e., the I-V profile) obtained (blue dashed line with squares). With no current flowing through an external load, the open circuit potential was 0.9 V. As the current was increased, there was a linear region where ohmic losses lowered the voltage. At a certain point, the voltage dropped more abruptly because of mass-transfer limitations. These losses are due to the fact that reactants did not reach the electrocatalytic sites [29].

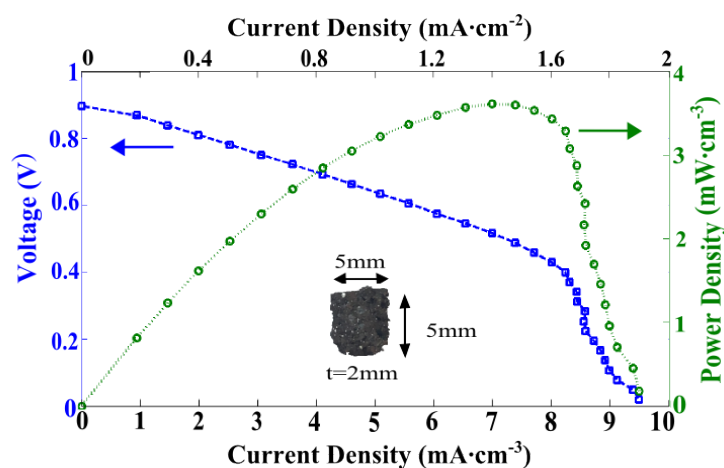


Figure 4. Performance measured for the SPGE (see also Figure 1C) when immersed in a 20 mM glucose solution: polarization curve (blue dashed line with squares) and power curve (green dotted line with circles).

When normalizing with respect to the electrode projected surface area (PSA)—namely only the rectangular base footprint of the SPGE is considered [30,31]—the highest surface power density reached was $\approx 720 \mu\text{W}\cdot\text{cm}^{-2}$ at $\approx 1400 \mu\text{A}\cdot\text{cm}^{-2}$ and 0.51 V (for the sake of clarity, only the surface current density is shown in Figure 4).

Performance evaluations based on the PSA, however, can be untrue (see the discussion in [30]). Here, it appears of limited significance because it completely neglects the porosity of the SPGE. Furthermore, trace amounts of Galinstan also appeared along the side edges where the scalpel blade was used to cut the SPGE. Therefore, PG also tended to grow along the thickness of the walls (2 mm) of the SPGE. Unfortunately, the PSA does not provide information with regard to the true three-dimensional nature of the SPGE, including its thickness. As in [30], we believe it is here more representative to rather consider the performance of the SPGE in terms of volumetric densities. In this case, the power density achieved was $\approx 3.6 \text{ mW}\cdot\text{cm}^{-3}$ at $\approx 7 \text{ mA}\cdot\text{cm}^{-3}$ and 0.51 V. Importantly, and independent of the normalized values favored, the net electrical power generated by the SPGE was almost $180 \mu\text{W}$. It was previously demonstrated that a net power of $105 \mu\text{W}$ generated at 0.35 V can already be exploited to drive a cardiac pacemaker [21]. Because the fabrication process presented in this communication appears easily scalable, we envision the possibility to use PDMS/Galinstan to create PG electrodes with different dimensions that might be able to supply power to a variety of (flexible) low-consumption electronic systems (e.g., implantables, wearables, but also wireless sensors, etc.).

4. Conclusions

Porous PDMS/Galinstan composites might open new perspectives for non-enzymatic glucose fuel cells. In this communication, we have shown that such composites can be utilized to create innovative electrodes. Two particular attributes of porous PDMS/Galinstan composites fabricated as presented in this communication can be highlighted: (i) unlike Galinstan inclusions in flat (i.e., non-porous) PDMS sheets, electrical conductivity can be achieved without mechanical sintering; (ii) they can be used as a support to grow complex and highly catalytic gold structures. To the best of our knowledge, the possibility to grow PG on such flexible elastomeric matrices has not been reported with the

more established HAET. The first tests conducted with an electrode immersed in a 20 mM glucose solution demonstrated the possibility to generate up to $\approx 3.6 \text{ mW}\cdot\text{cm}^{-3}$ at 0.51 V without using any enzymes. Further research is now required to study the repeatability of the fabrication process. In the near future, we also plan to assess more thoroughly the mechanical, electrical and electrochemical properties of the new material. In this perspective, we are currently assembling a dedicated platform to accurately bend and/or stretch the PDMS/Galinstan composite (with and without PG) in a repeatable manner. Experiments are also on-going to further investigate the performance of the material at lower glucose concentrations (e.g., 3.5–10 mM), as well as at different temperatures (e.g., body temperature). Additionally, cyclic voltammetry tests and experiments over long periods of time will be carried out soon. Finally, PG electrodes of different dimensions will be evaluated. Because the fabrication process reported appears easily scalable, we indeed envision PG electrodes with long-term stability that might meet the power budget of a plurality of low-consumption electronic devices.

Author Contributions: Conceptualization, D.D.; investigation, D.D., F.L.M. and A.Q.; writing, original draft preparation, D.D.; writing, review and editing, D.D., F.L.M, F.R., A.Q. and M.D.V.; supervision, F.R. and M.D.V.; project administration, F.R. and M.D.V.

Funding: This research received no external funding.

Conflicts of Interest: The authors declare no conflict of interest.

References

1. Liu, Y.; Pharr, M.; Salvatore, G.A. Lab-on-skin: A review of flexible and stretchable electronics for wearable health monitoring. *ACS Nano* **2017**, *11*, 9614–9635. [[CrossRef](#)] [[PubMed](#)]
2. Bandothkar, A.J.; Wang, J. Wearable biofuel cells: A review. *Electroanalysis* **2016**, *28*, 1188–1200. [[CrossRef](#)]
3. Bandothkar, A.J. Wearable biofuel cells: Past, present and future. *J. Electrochem. Soc.* **2017**, *164*, H3007–H3014. [[CrossRef](#)]
4. Gonzalez-Solino, C.; Lorenzo, M.D. Enzymatic fuel cells: Towards self-powered implantable and wearable diagnostics. *Biosensors* **2018**, *8*, 11. [[CrossRef](#)] [[PubMed](#)]
5. Bandothkar, A.J.; You, J.M.; Kim, N.H.; Gu, Y.; Kumar, R.; Mohan, A.V.; Kurniawan, J.; Imani, S.; Nakagawa, T.; Parish, B.; et al. Soft, stretchable, high power density electronic skin-based biofuel cells for scavenging energy from human sweat. *Energy Environ. Sci.* **2017**, *10*, 1581–1589. [[CrossRef](#)]
6. Jia, W.; Valdés-Ramírez, G.; Bandothkar, A.J.; Windmiller, J.R.; Wang, J. Epidermal biofuel cells: Energy harvesting from human perspiration. *Angew. Chem. Int. Ed.* **2013**, *52*, 7233–7236. [[CrossRef](#)] [[PubMed](#)]
7. Zebda, A.; Gondran, C.; Le Goff, A.; Holzinger, M.; Cinquin, P.; Cosnier, S. Mediatorless high-power glucose biofuel cells based on compressed carbon nanotube-enzyme electrodes. *Nat. Commun.* **2011**, *2*, 370. [[CrossRef](#)] [[PubMed](#)]
8. Falk, M.; Andoralov, V.; Blum, Z.; Sotres, J.; Suyatin, D.B.; Ruzgas, T.; Arnebrant, T.; Shleev, S. Biofuel cell as a power source for electronic contact lenses. *Biosens. Bioelectron.* **2012**, *37*, 38–45. [[CrossRef](#)] [[PubMed](#)]
9. Moehlenbrock, M.J.; Minteer, S.D. Extended lifetime biofuel cells. *Chem. Soc. Rev.* **2008**, *37*, 1188–1196. [[CrossRef](#)] [[PubMed](#)]
10. Calabrese Barton, S.; Gallaway, J.; Atanassov, P. Enzymatic biofuel cells for implantable and microscale devices. *Chem. Rev.* **2004**, *104*, 4867–4886. [[CrossRef](#)]
11. Du Toit, H.; Di Lorenzo, M. Electrodeposited highly porous gold microelectrodes for the direct electrocatalytic oxidation of aqueous glucose. *Sens. Actuators B* **2014**, *192*, 725–729. [[CrossRef](#)]
12. Cherevko, S.; Chung, C.H. Direct electrodeposition of nanoporous gold with controlled multimodal pore size distribution. *Electrochem. Commun.* **2011**, *13*, 16–19. [[CrossRef](#)]
13. Sanzó, G.; Taurino, I.; Antiochia, R.; Gorton, L.; Favero, G.; Mazzei, F.; De Micheli, G.; Carrara, S. Bubble electrodeposition of gold porous nanocorals for the enzymatic and non-enzymatic detection of glucose. *Bioelectrochemistry* **2016**, *112*, 125–131. [[CrossRef](#)] [[PubMed](#)]
14. Cheng, S.; Wu, Z. Microfluidic electronics. *Lab. Chip* **2012**, *12*, 2782–2791. [[CrossRef](#)] [[PubMed](#)]
15. Sivan, V.; Tang, S.Y.; O'Mullane, A.P.; Petersen, P.; Eshtiaghi, N.; Kalantar-zadeh, K.; Mitchell, A. Liquid metal marbles. *Adv. Funct. Mater.* **2013**, *23*, 144–152. [[CrossRef](#)]

16. Miao, Y.E.; Lee, H.K.; Chew, W.S.; Phang, I.Y.; Liu, T.; Ling, X.Y. Catalytic liquid marbles: Ag nanowire-based miniature reactors for highly efficient degradation of methylene blue. *Chem. Commun.* **2014**, *50*, 5923–5926. [[CrossRef](#)] [[PubMed](#)]
17. Liang, S.; Rao, W.; Song, K.; Liu, J. Fluorescent Liquid Metal as a Transformable Biomimetic Chameleon. *ACS Appl. Mater. Interfaces* **2018**, *10*, 1589–1596. [[CrossRef](#)] [[PubMed](#)]
18. Hoshyargar, F.; Crawford, J.; O' Mullane, A.P. Galvanic replacement of the liquid metal galinstan. *J. Am. Chem. Soc.* **2016**, *139*, 1464–1471. [[CrossRef](#)] [[PubMed](#)]
19. Fassler, A.; Majidi, C. Liquid-phase metal inclusions for a conductive polymer composite. *Adv. Mater.* **2015**, *27*, 1928–1932. [[CrossRef](#)] [[PubMed](#)]
20. Zimmet, P.; Alberti, K.; Shaw, J. Global and societal implications of the diabetes epidemic. *Nature* **2001**, *414*, 782–787. [[CrossRef](#)] [[PubMed](#)]
21. Holade, Y.; MacVittie, K.; Conlon, T.; Guz, N.; Servat, K.; Napporn, T.W.; Kokoh, K.B.; Katz, E. Pacemaker activated by an abiotic biofuel cell operated in human serum solution. *Electroanalysis* **2014**, *26*, 2445–2457. [[CrossRef](#)]
22. Kerzenmacher, S.; Ducrée, J.; Zengerle, R.; Von Stetten, F. Energy harvesting by implantable abiotically catalyzed glucose fuel cells. *J. Power Sources* **2008**, *182*, 1–17. [[CrossRef](#)]
23. Slaughter, G.; Sunday, J. A membraneless single compartment abiotic glucose fuel cell. *J. Power Sources* **2014**, *261*, 332–336. [[CrossRef](#)]
24. Desmaële, D.; La Malfa, F.; Rizzi, F.; Qualtieri, A.; Di Lorenzo, M.; De Vittorio, M. A novel flexible conductive sponge-like electrode capable of generating electrical energy from the direct oxidation of aqueous glucose. *J. Phys. Conf. Ser.* **2018**, in press.
25. Lin, Y.; Cooper, C.; Wang, M.; Adams, J.J.; Genzer, J.; Dickey, M.D. Handwritten, soft circuit boards and antennas using liquid metal nanoparticles. *Small* **2015**, *11*, 6397–6403. [[CrossRef](#)] [[PubMed](#)]
26. Wang, L.; Liu, C.H.; Nemoto, Y.; Fukata, N.; Wu, K.C.W.; Yamauchi, Y. Rapid synthesis of biocompatible gold nanoflowers with tailored surface textures with the assistance of amino acid molecules. *RSC Adv.* **2012**, *2*, 4608–4611. [[CrossRef](#)]
27. Xu, F.; Cui, K.; Sun, Y.; Guo, C.; Liu, Z.; Zhang, Y.; Shi, Y.; Li, Z. Facile synthesis of urchin-like gold submicrostructures for nonenzymatic glucose sensing. *Talanta* **2010**, *82*, 1845–1852. [[CrossRef](#)] [[PubMed](#)]
28. Liu, A.; Ren, Q.; Xu, T.; Yuan, M.; Tang, W. Morphology-controllable gold nanostructures on phosphorus doped diamond-like carbon surfaces and their electrocatalysis for glucose oxidation. *Sens. Actuators B* **2012**, *162*, 135–142. [[CrossRef](#)]
29. Weber, A.Z.; Newman, J. Modeling transport in polymer-electrolyte fuel cells. *Chem. Rev.* **2004**, *104*, 4679–4726. [[CrossRef](#)] [[PubMed](#)]
30. Flexer, V.; Brun, N.; Courjean, O.; Backov, R.; Mano, N. Porous mediator-free enzyme carbonaceous electrodes obtained through integrative chemistry for biofuel cells. *Energy Environ. Sci.* **2011**, *4*, 2097–2106. [[CrossRef](#)]
31. Tsujimura, S.; Kamitaka, Y.; Kano, K. Diffusion-controlled oxygen reduction on multi-copper oxidase-adsorbed carbon aerogel electrodes without mediator. *Fuel Cells* **2007**, *7*, 463–469. [[CrossRef](#)]



© 2018 by the authors. Licensee MDPI, Basel, Switzerland. This article is an open access article distributed under the terms and conditions of the Creative Commons Attribution (CC BY) license (<http://creativecommons.org/licenses/by/4.0/>).